Marginally unstable Holmboe modes

Alexandros Alexakis
Laboratoire Cassiopée, Observatoire de la Côte d'Azur, Boite Postale 4229, Nice Cedex 04, France and National Center for Atmospheric Research, Boulder, Colorado 80305

(Received 30 October 2006; accepted 15 March 2007; published online 15 May 2007)

Marginally unstable Holmboe modes for smooth density and velocity profiles are studied. For a large family of flows and stratification that exhibit Holmboe instability, it is shown that the modes with phase velocity equal to the maximum or the minimum velocity of the shear are marginally unstable. This allows us to determine the critical value of the control parameter R (expressing the ratio of the velocity variation length scale to the density variation length scale) above which Holmboe instability is present, $R_{\text{crit}}=2$. Furthermore, systems for which the parameter R is very close to this critical value R_{crit} are examined. For this case, an analytical expression for the dispersion relation of the complex phase speed $c(k)$ in the unstable region is derived. The growth rate and the width of the region of unstable wavenumbers has a very strong (exponential) dependence on the deviation of R from the critical value. Two specific examples are examined and a physical interpretation of the results is described. © *2007 American Institute of Physics*.
[DOI: 10.1063/1.2730545]

I. INTRODUCTION

Holmboe instability in stratified shear flows appears in a variety of physical contexts such as in astrophysics, the Earth's atmosphere, and oceanography.[1–9] Although the typical growth rate is smaller than that of Kelvin-Helmholtz instability, it is present for arbitrarily large values of the global Richardson number making Holmboe instability a good candidate for the generation of turbulence and mixing in many physical scenarios.

What distinguishes Holmboe from the Kelvin-Helmholtz instability is that unlike the latter instability, the Holmboe unstable modes have nonzero phase velocity that depends on the wavenumber (i.e., traveling dispersive modes). It was first identified by Holmboe[10] in a simplified model of a continuous piecewise linear velocity profile and a step-function density profile. Several authors have expanded Holmboe's theoretical work[11–14] by considering different stratification and velocity profiles that do not include the simplifying symmetries Holmboe used in his model. Hazel[15] and more recently Smyth and Peltier[16] and Alexakis[17] have shown that Holmboe's results hold for smooth density and velocity profiles as long as the length scale of the density variation is sufficiently smaller than the length scale of the velocity variation. Furthermore, effects of viscosity and diffusivity,[18,19] nonlinear evolution,[20–23] and mixing properties[24] of the Holmboe instability have also been investigated. The predictions of Holmboe have also been tested experimentally. Browand and Winant[25] first performed shear flow experiments in a stratified environment under conditions for which Holmboe's instabilities are present. Their investigation has been extended further by more recent experiments.[11,26–32]

Although the understanding of Holmboe instability has progressed a lot since the time of Holmboe, there are still basic theoretical questions that remain unanswered, even in the linear theory. Most of the work for the linear stage of the instability has been based on the Taylor-Goldstein (TG) equation (see Ref. 33), which describes linear normal modes of a parallel shear flow in a stratified, inviscid, nondiffusive, Boussinesq fluid:

$$\frac{d^2\phi}{dz^2}-\left[k^2+\frac{U''}{U-c}-\frac{J(z)}{(U-c)^2}\right]\phi=0, \tag{1}$$

where $\phi(z)$ is the complex amplitude of the stream function for a normal mode with real wavenumber k. c is the complex phase velocity. $\text{Im}\{c\}>0$ implies instability with growth rate given by $\zeta=k\text{Im}\{c\}$. $U(z)$ is the unperturbed velocity in the x direction. $J(z)=-g\rho'/\rho$ is the squared Brunt-Väisälä frequency where ρ is the unperturbed density stratification and g is the acceleration of gravity. The prime on the unperturbed quantities indicates differentiation with respect to z. Equation (1) together with the boundary conditions $\phi\to 0$ for $z\to\pm\infty$ forms an eigenvalue problem for the complex eigenvalue c.

Here, a few known results for the Taylor-Goldstein equation are presented, and some results for Holmboe's instability are reviewed, in order to help the reader with the mathematical derivations and the discussion that follow in the next sections. If c is real and in the range of U, there is a height z_c at which $U(z_c)=c$. At this height z_c, called the critical height, Eq. (1) has a regular singular point. For some conditions, unstable modes exist with the real part of the phase velocity within the range of U. The phase speed of these modes satisfies Howard's semicircle theorem, $|c-1/2(\sup\{U\}+\inf\{U\})|<1/2|\sup\{U\}-\inf\{U\}|$. If these unstable modes exist, the Miles-Howard theorem[34] guarantees that somewhere in the flow the local Richardson number defined by

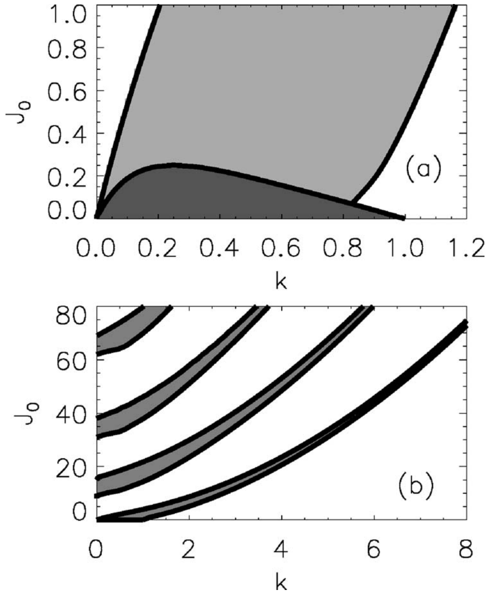

FIG. 1. Stability diagram for the Hazel model for $R=3$. Panel (a) shows the Kelvin-Helmholtz unstable region with dark gray, and the Holmboe unstable region with light gray. In the Kelvin-Helmholtz region, unstable nontraveling modes ($\mathrm{Re}\{c\}=0$) exist. The boundary of this region is composed of neutral modes with $c=0$. In the Holmboe unstable region, on the other hand, unstable dispersive modes exist with $0<|\mathrm{Re}\{c\}|<1$. The left stability boundary of this region is composed of modes with $c=1$, and the right stability boundary is composed of singular neutral modes with $0<c<1$. On the left of the Holmboe unstable region, stable gravity waves exist with $|c|>1$ and on the right of the Holmboe unstable region neutral singular modes exist with $|c|<1$. Panel (b) shows the same instability diagram for larger values of J_0. For sufficiently large J_0, more than one Holmboe unstable region exists. These new unstable modes are related to the higher harmonics of the internal gravity wave spectrum.

$$\mathrm{Ri}(z)=\frac{J(z)}{[U'(z)]^2} \tag{2}$$

must be smaller than $1/4$.

Equation (1) has been shown to give rise to Kelvin-Helmholtz and Holmboe unstable modes for a variety of velocity and density profiles. An example that captures both kinds of instabilities (introduced originally by Hazel in Ref. 15) assumes a velocity profile given by $U(z)=\tanh(z)$ and the squared Brunt-Väisälä frequency being given by $J=J_0\cosh(Rz)^{-2}$, where J_0 is the global Richardson number defined here as $J_0\equiv\mathrm{Ri}(0)$. This example (from now on called the "Hazel model") has been used in many studies, and is going to be used as the basic example in the current work to illustrate the more general results derived in the following sections. It is useful for this reason to describe it in some detail.

The case of $R=1$ was examined by Miles[35] analytically and numerically by Hazel.[15] It exhibits only Kelvin-Helmholtz instability for the wavenumbers that satisfy $k(1-k)>J_0$. Hazel[15] also examined numerically the case $R=5$ in which it was shown that along with the Kelvin-Helmholtz unstable region, there is also a stripe (in a J_0-k diagram) of unstable Holmboe modes. As an example, the instability region for $R=3$ is shown in Fig. 1(a). In this case, the J_0-k plane is divided into four regions. The Kelvin-Helmholtz unstable region consists of unstable modes with $\mathrm{Re}\{c\}=0$ and is restricted in the finite region shown in Fig. 1(a) (marked with dark gray). The boundary of this region is composed of modes with $c=0$ (see Refs. 15 and 35). The Holmboe unstable region forms a semi-infinite stripe in the diagram and is present for arbitrary large values of the global Richardson number J_0 (marked with light gray in Fig. 1). The unstable modes in this region are dispersive with phase velocity satisfying $0<|c|<1$. At that time of Hazel's[15] investigation, the kind of modes that determine the boundaries were not determined. The two regions on the left and on the right of the Holmboe instability stripe are stable and consist of stable gravity waves and singular modes that are part of the continuous spectrum.[39,40]

Hazel observed that if $R>2$, there is always a height at which the local Richardson number $\mathrm{Ri}(z)=J_0\cosh(z)^4/\cosh(Rz)^2$ is smaller than $1/4$. Based on this observation, Hazel conjectured that $R=2$ is the critical value of R above which the Holmboe instability appears. Later careful numerical examination by Smyth[16] found unstable Holmboe modes to appear only for values of R larger than $R>2.4$. More recently, Alexakis[17] showed that the instability can be found for smaller values of R up to $R=2.2$, making the conjecture by Hazel still plausible. It is worth noting that the width of the Holmboe instability stripe and the growth rate of the modes decrease as the control parameter R is approaching the value 2 from above, making the detection of the Holmboe unstable modes with a numerical code difficult.

More specifically, Alexakis[17] showed (numerically) for the Hazel model that the left instability boundary of the Holmboe instability region [see Fig. 1(a)] is composed of marginally unstable modes with phase velocity equal to the maximum or the minimum of the shear velocity. Such a condition has been known to hold for smooth velocity and discontinuous density profiles.[36–38] Finding these marginally unstable modes corresponds to solving for the energy states $E=-k^2$ in a Schrödinger problem for a particle in a potential well,

$$\frac{d^2\phi}{dz^2}-[k^2+V_c(z)]\phi=0, \tag{3}$$

where

$$V_c(z)=\frac{U''}{U-c}-\frac{J(z)}{(U-c)^2} \tag{4}$$

and c is taken to be $c=U_{\mathrm{max/min}}$, the maximum or minimum velocity of the shear layer. Note that the modes $c=U_{\mathrm{max/min}}$ do not always exist. For the Hazel model, for example, these modes exist only if $R\geqslant 2$ (see Ref. 17). The right boundary of the Holmboe unstable region, on the other hand [see Fig. 1(a)], is composed of singular modes with phase velocity within the range of the shear velocity. These modes can be determined by imposing the condition that the solution close to the critical height can be expanded in terms of only one of the two corresponding Frobenius solutions (see Ref. 17).

Furthermore, it was shown that for sufficiently large J_0, more than one instability stripe exists. These new instability stripes are related with the higher internal gravity modes of the unforced system, and their right instability boundaries are determined by the higher eigenstates in the Schrödinger problem (3). Figure 1(b) shows the instability region for $R=3$ and J_0 up to 80. We note that different unstable Holmboe modes have been found experimentally in Ref. 32 that were then interpreted in terms of the multilayer model of Ref. 12.

The physical picture, described in Ref. 17, for the Holmboe instability is as follows. For sufficiently small wavenumbers, the solutions of the TG equation include a discrete number of stable gravity waves with phase velocity larger than the velocity of the shear. As the wavenumber is increased, the phase speed of these modes decreases approaching the maximum value of the velocity of the shear. If the stratification length scale is small enough, there is a critical wavenumber k_0 for which the phase velocity of the waves becomes equal to the maximum wind velocity. This corresponds to the left instability boundary of the Holmboe unstable region. For wavenumbers larger than k_0, the phase velocity of the gravity waves is smaller than the maximum wind velocity and the modes become unstable. The instability persists up to another critical value of the wavenumber $k=k_s$, for which the growth rate is zero but the real part of the phase velocity is within the range of U. The mode with this wavenumber exhibits a singular behavior at the critical height and determines the right instability boundary of the Holmboe unstable region. For wavenumbers smaller than k_s, a continuum of singular neutral modes exists.

The understanding, however, of the linear part of Holmboe instability for smooth shear and density profiles still remains conjectural and most of the results are based on numerical calculations, therefore they do not constitute proofs. This work attempts to address some of these issues. In the next section, it is proven for a general class of velocity profiles that the modes that have phase velocity equal to the maximum/minimum velocity of the shear are marginally unstable. Section III examines the case for which the parameter R is slightly larger than its critical value, and the dispersion relation inside the instability region is derived based on an asymptotic expansion. In Sec. IV, these results are tested for specific shear and density profiles. A summary of the results, their physical interpretation, and the final conclusions are in Sec. V.

II. MARGINAL WAVENUMBER

In this section, for a general family of flows the modes with phase velocity equal to the maximum/minimum velocity of the flow are examined with the aim of determining under what conditions these modes constitute a stability boundary.

Consider an infinite shear layer specified by the monotonic velocity profile $U(y)$ that has the asymptotic values $U(\pm\infty)=U_{\pm\infty}$. Since the system is Galilean invariant with no loss of generality, we can set $U_{+\infty}=-U_{-\infty}=U_\infty$. More precisely, we will assume that the asymptotic behavior of $U(y)$ for $y\rightarrow+\infty$ is going to be given by

$$U(y) \simeq U_\infty - U^* e^{-\alpha y}. \qquad (5)$$

The layer is stably stratified with $J(y)>0$ having asymptotic behavior $J(y)\simeq J^* e^{-\beta y}$ for $y\rightarrow+\infty$. In what follows, we are going to concentrate only on the modes with phase velocity close to $c=U_\infty$; the results can easily be reproduced for the $c=U_{-\infty}$ modes by following the same arguments.

At this stage, it is useful to rescale the variables in the TG equation using the maximum velocity U_∞ and the length scale α^{-1}. The new vertical coordinate now becomes $y=\alpha z$. The wavenumber becomes $q=k/\alpha$ and c is measured in units of U_∞. The resulting nondimensional control parameters for our system are the ratio of the two velocities, $\sigma\equiv U^*/U_\infty$; the asymptotic Richardson number, $J_\infty\equiv J^*/(U^*\alpha)^2 = J^*/(\sigma U_\infty \alpha)^2$; and the ratio of the two length scales, $R\equiv\beta/\alpha$. To avoid introducing more symbols, the same symbol for the functions U, J, ϕ, V_c is going to be used for both coordinates z and y. The velocity profile in the z coordinates $U(z)=U_\infty-U^*e^{-\alpha z}$ becomes in the y coordinates $U(y)=1-\sigma e^{-y}$ and $J(z)=J^*e^{-\beta z}$ becomes $J(y)=\sigma^2 J_\infty e^{-Ry}$ (without introducing a new symbol for U and J as a strict mathematical formulation would demand). For example, in the Hazel model $\alpha=2$ and $U_\infty=1$ and the velocity profile becomes $U(y)=\tanh(y/\alpha)/U_\infty=\tanh(y/2)$ and $J(y)=(J_0/\alpha^2U_\infty^2)\cosh^{-2}(Ry/\alpha)=\sigma^2 J_\infty \cosh^{-2}(Ry/2)$. Note that $J(z)$ has units of $[\text{velocity}]^2/[\text{length}]^2$ and needs to be rescaled by $\alpha^2 U_\infty^2$, and V_c has units of $[\text{length}]^{-2}$ and needs to be rescaled by α^2. The TG equation (1) in the new coordinates system for the large values of y becomes

$$\frac{d^2\phi}{dy^2} - \left[q^2 - \frac{\sigma e^{-y}}{1-\sigma e^{-y}-c} - \frac{\sigma^2 J_\infty e^{-Ry}}{(1-\sigma e^{-y}-c)^2}\right]\phi = 0. \qquad (6)$$

Let us assume that a solution $\phi_0(y)$ of the Schrödinger problem described in Eq. (3) for the wavenumber $q_0=k_0/\alpha$ exists. Note that for large y and for $c=1$, the potential $V_c(y)$ has the behavior $V_c(y)\simeq 1-J_\infty e^{-(R-2)y}$. Clearly, if $R>2$ the asymptotic behavior of V_c for large y is $V_c(y)\simeq 1$ and $\phi_0(y)$ behaves as $\phi\sim\varphi_\infty e^{-\lambda y}$ with $\lambda=\sqrt{q^2+1}$. If, however, we have $R=2$, then $V_c(y)\simeq 1-J_\infty$ for $y\rightarrow\infty$ and $\lambda=\sqrt{q^2+1-J_\infty}$. For abbreviation denote for both cases

$$\lambda = \sqrt{q^2+1-\tilde{J}}, \qquad (7)$$

where $\tilde{J}$ (that will be defined precisely later on) takes the values $\tilde{J}\simeq 0$ when $R>2$ and $\tilde{J}=J_\infty$ when $R=2$. As discussed in Ref. 17, no solution exists that satisfies the boundary conditions for the Schrödinger problem described in Eq. (3) if $R<2$ since it corresponds in finding bounded eigenstates in an unbounded potential well.

The aim in this section is to find how c changes from the value 1 as we increase q from the value q_0. We proceed by carrying out a regular asymptotic expansion by letting $q=q_0+\epsilon q_1$ and $c=1-\epsilon c_1+\cdots$ with $0<\epsilon\ll 1$ and c_1 in general complex. However, as we deviate from the $c=1$ case, the behavior of the potential $V_c(y)$ drastically changes $[\mathcal{O}(1)$ change$]$ in the large y region and only slightly (linearly with respect to the change in c) for $y\simeq\mathcal{O}(1)$. Figure 2 illustrates this change for the Hazel model. This implies that two different expansions are needed, one for y being of $\mathcal{O}(1)$ and one for large y.

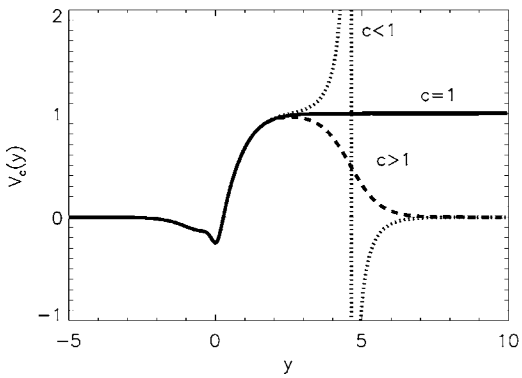

FIG. 2. The potential $V_c(y)$ for the Hazel model with $R=3$ and $J_0=1$ for three values of c, $c=1$ (solid line), $c=1+\epsilon$ (dashed line), and $c=1-\epsilon$ (dotted line), where $0<\epsilon \ll 1$. For $c=1 V_c(y)$, asymptotes to the value $V_c \simeq 1$. This behavior drastically changes when $c\neq 1$. For $c<1 V_c(y)$, there is a singularity at $U(y)=c$ and asymptotes to 0. For $c>1 V_c(y)$, there is no singularity but asymptotes to 0 for sufficiently large y. Note that the potential $V_c(z)$ has units $[\text{length}]^{-2}$ and has been rescaled by $\alpha^2=4$ to obtain $V_c(y)$.

A. Local solution: $y=\mathcal{O}(1)$

Starting with the local solution and expanding ϕ as $\phi=\phi_0+\epsilon\phi_1+\cdots$ for $y=\mathcal{O}(1)$ results at first order in the equation

$$\frac{d^2\phi_1}{dy^2}-[q_0^2+V_0(y)]\phi_1=[2q_1q_0-c_1V_1(y)]\phi_0, \tag{8}$$

where $V_0=V_c$ is given in Eq. (4) for $c=1$ and

$$V_1(y)=\left.\frac{\partial}{\partial c}\left[\frac{U''}{U-c}-\frac{J(y)}{(U-c)^2}\right]\right|_{c=1} =\frac{U''}{(U-1)^2}-\frac{2J(y)}{(U-1)^3}.$$

The solution of this inhomogeneous equation can be found using the Wronskian to obtain

$$\phi_1=\phi_0(y)\int_0^y\frac{\int_{-\infty}^{y'}[2q_1q_0-c_1V_1(y'')]\phi_0^2(y'')dy''}{\phi_0^2(y')}dy', \tag{9}$$

where the normalization condition $\phi(0)=\phi_0(0)$ is chosen. Clearly this solution satisfies the boundary condition for $y\to-\infty$. For $y\to+\infty$, by performing the integrations, we obtain

$$\phi_1\simeq\frac{2q_1q_0I_1-c_1I_2}{2\lambda\varphi_\infty}e^{\lambda y}+\mathcal{O}(e^{-\lambda y}), \tag{10}$$

where $I_1=\int_{-\infty}^{+\infty}\phi_0^2dy>0$ and $I_2=\int_{-\infty}^{+\infty}V_1\phi_0^2dy$. Here we need to assume that the integral I_2 exists and is finite. Note that if $V_1(y)$ is not singular, $|I_2|<\infty$ for $R>2$, but $|I_2|<\infty$ only if $\lambda>1/2$ for $R=2$. The $\mathcal{O}(e^{-\lambda y})$ terms can be neglected when compared with ϕ_0 but not the $\mathcal{O}(e^{\lambda y})$ terms since for sufficiently large y they can become important.

So the large y behavior of ϕ based on the local solution is given by

$$\phi\simeq\varphi_\infty e^{-\lambda y}+\epsilon\frac{2q_1q_0I_1-c_1I_2}{2\lambda\varphi_\infty}e^{\lambda y}+\cdots. \tag{11}$$

B. Far away solution: $y=\mathcal{O}(\ln[1/\epsilon])$

As discussed at the beginning of this section, the behavior of $V_c(y)$ drastically changes when $c\neq 1$ [$\mathcal{O}(1)$ change] for large values of y. In particular, the TG equation (6) for large values of y and for $c=1-\epsilon c_1$ reads

$$\frac{d^2\phi}{dy^2}-\left[q^2-\frac{\sigma}{\epsilon c_1e^y-\sigma}-\frac{\sigma^2J_\infty e^{-(R-2)y}}{(\epsilon c_1e^y-\sigma)^2}\right]\phi=0. \tag{12}$$

For y of $\mathcal{O}(1)$, this expression reduces to the case $c=1$ to first order. This is no longer true when the denominators in the above equation are close to zero (i.e., $\epsilon c_1e^y\sim\sigma$). To capture, therefore, the large y behavior, we need to make the change of variables $\tilde{y}=y-y_c$, where $y_c=-\ln(\epsilon c_1/\sigma)$ is the location of the singularity determined by $U(y_c)=c$. (Note that for c_1 complex, $\tilde{y}$ does not coincide with the real y axis.) The Taylor-Goldstein equation (1) then reads

$$\frac{d^2\phi}{d\tilde{y}^2}-\left[q^2-\frac{1}{e^{\tilde{y}}-1}-\frac{J_\infty\cdot\left(\frac{\epsilon c_1}{\sigma}\right)^\delta\cdot(e^{-\tilde{y}})^\delta}{(e^{\tilde{y}}-1)^2}\right]\phi=0, \tag{13}$$

where $\delta=R-2$ and only the leading terms have been kept. Introducing the variable $s=e^{-\tilde{y}}$ leads to

$$s^2\frac{d^2}{ds^2}\phi+s\frac{d}{ds}\phi-\left[q^2-\frac{s}{1-s}-\frac{\tilde{J}s^2s^\delta}{(1-s)^2}\right]\phi=0, \tag{14}$$

where $\tilde{J}=J_\infty\cdot(\epsilon c_1/\sigma)^\delta$ is the Richardson number at the critical height. Note that if $R=2$ (i.e., $\delta=0$), then $\tilde{J}=J_\infty=\mathcal{O}(1)$. If, however, $R>2$, then $\tilde{J}\ll 1$ and the term in the brackets proportional to $\tilde{J}$ is small and can be neglected everywhere except close to the singularity $s=1$. To deal with this small singular term, we can write for s close to 1, $s^\delta\simeq 1-\delta(1-s)+\cdots$, and keep the leading term. That way the principal term inside the brackets is always kept for all values of s and our solution will be correct to first order for all values of $R\geqslant 2$ by solving

$$s^2\frac{d^2}{ds^2}\phi+s\frac{d}{ds}\phi-\left[q^2-\frac{s}{1-s}-\frac{\tilde{J}s^2}{(1-s)^2}\right]\phi=0. \tag{15}$$

To deal with the singularities at $s=0$ and 1, we can make the substitution $\phi=s^q(1-s)^\mu h(s)$ with $\mu=1/2-\sqrt{1/4-\tilde{J}}$. This leads to the hypergeometric equation

$$s(1-s)\frac{d^2}{ds^2}h+[(2q+1)-(2\mu+2q+1)s]\frac{d}{ds}h +[1-\mu-(q+1)]h=0, \tag{16}$$

the solution of which is the hypergeometric function $h(s)=F(a,b,d;s)$ with

$$a=(\mu+q)+\sqrt{q^2+1-\tilde{J}},$$

$$b=(\mu+q)-\sqrt{q^2+1-\tilde{J}},$$

and

$$d=(2q+1).$$

Note that $q+\mu-a=-\lambda$ and $q+\mu-b=+\lambda$. Some basic properties of the hypergeometric function are given in Appendix A; here only the resulting asymptotic behavior of ϕ is given,

$$\lim_{s\to 0} \phi \simeq s^q = e^{-qy}, \tag{17}$$

$$\lim_{s\to+\infty} \phi \simeq \frac{\Gamma(d)\Gamma(b-a)}{\Gamma(b)\Gamma(d-a)} s^q(-s)^{\mu-a} + \frac{\Gamma(d)\Gamma(a-b)}{\Gamma(a)\Gamma(d-b)} s^q(-s)^{\mu-b}. \tag{18}$$

Returning to the y variable and up to a normalization factor A, the asymptotic behavior of ϕ for $y \ll y_c$ is

$$\phi \simeq A\left[e^{-\lambda y} + (-\epsilon c_1)^{2\lambda} \frac{\Gamma(a)\Gamma(d-b)\Gamma(-2\lambda)}{\Gamma(b)\Gamma(d-a)\Gamma(2\lambda)} e^{\lambda y}\right]. \tag{19}$$

C. Matching

Matching the exponentially decreasing terms of the local and the faraway solution, we obtain $A=\varphi_\infty$, and from the exponentially increasing terms we have

$$\epsilon\frac{2q_1q_0I_1-c_1I_2}{2\lambda\varphi_\infty} = \varphi_\infty(-\epsilon c_1)^{2\lambda}\frac{\Gamma(a)\Gamma(d-b)\Gamma(-2\lambda)}{\Gamma(b)\Gamma(d-a)\Gamma(2\lambda)}. \tag{20}$$

The equation above can be solved iteratively by letting $\epsilon c_1 = \epsilon c_1' + \epsilon^{2\lambda} c_2' + \cdots$. To first order, we obtain

$$c_1' = \frac{2q_1q_0I_1}{I_2}, \tag{21}$$

which gives the first correction to the phase speed and determines if the real part of phase speed is increasing or decreasing with the wavenumber. If, for example, $I_2>0$ (which will be the case in the examples that follow), then c is decreasing with q and the correction c_1' is positive for positive q_1 and negative for negative q_1. The opposite holds if $I_2<0$. From now on we will assume that $I_2>0$, which is the physically expected case (Re$\{c(k)\}$ being a decreasing function of k; for example, a step function density profile gives $c\sim 1/\sqrt{k}$). If, however, there is a velocity and density profile such that $I_2<0$, the same results will hold but for the opposite direction in q (i.e., wavenumbers smaller than q_0 will be unstable and wavenumbers larger than q_0 will be stable). This first-order correction, however, is real, and contains no information about the growth rate. At the next order, we have

$$-\frac{c_2'I_2}{2\lambda\varphi_\infty} = \varphi_\infty(-c_1')^{2\lambda}\frac{\Gamma(a)\Gamma(d-b)\Gamma(-2\lambda)}{\Gamma(b)\Gamma(d-a)\Gamma(2\lambda)}. \tag{22}$$

This correction is much smaller but contains the first-order correction of the imaginary part of c. The dispersion relation of c for q close to q_0 can then be written in terms of q as

$$c = 1 - \frac{2q_0I_1}{I_2}(q-q_0) + \frac{2\lambda\varphi_\infty^2}{I_2}\left(\frac{-2k_0I_1}{I_2}(q-q_0)\right)^{2\lambda} \times\frac{\Gamma(a)\Gamma(d-b)\Gamma(-2\lambda)}{\Gamma(b)\Gamma(d-a)\Gamma(2\lambda)}. \tag{23}$$

Special care is needed to interpret the term $(-c_1')^{2\lambda}$ for c_1' given by Eq. (21). When $q_1<0$, c_1' is negative and the term $(-c_1')^{2\lambda}$ is real; this corresponds to the case in which c becomes larger than the shear velocity and no critical layer is formed. The Howard semicircle theorem then guarantees stability. This proves that wavenumbers slightly smaller than q_0 are stable. When $q_1>0$, c_1' is positive and $(-c_1')^{2\lambda}$ becomes a complex number that can take different values depending on whether the minus sign is interpreted as $e^{i\pi}$ or $e^{-i\pi}$. The choice depends on the location of the singularity on the complex plane when we integrate the Taylor-Goldstein equation (1). If Im$\{c_1\}>0$, then $(-c_1)^{2\lambda}$ should be interpreted as $|c_1|^{2\lambda}e^{-i2\lambda\pi}$ because the integration is going over the singularity. If Im$\{c_1\}<0$, then $(-c_1)^{2\lambda}$ should be interpreted as $|c_1|^{2\lambda}e^{+i2\lambda\pi}$ because the integration is going under the singularity. Here we arrive at an important point in the derivation: the sign of the imaginary part of c based on Eq. (23) depends on the original assumption about the sign of Im$\{c\}$ when the TG equation is integrated across the singularity. Thus, in order for the matching to be successful, we need to verify that the original assumption about the sign of Im$\{c_1\}$ is consistent with the final result. If we assume that Im$\{c_1\}>0$, then from (22) we have that

$$0<\mathrm{Im}\{c_1\} = \sin(2\lambda\pi)|c_1|^{2\lambda}\frac{2\lambda\varphi_\infty^2}{I_2}\frac{\Gamma(a)\Gamma(d-b)\Gamma(-2\lambda)}{\Gamma(b)\Gamma(d-a)\Gamma(2\lambda)}, \tag{24}$$

where Im$\{(c_1')^{2\lambda}\}$ is written as $-\sin(2\lambda\pi)|c_1|^{2\lambda}$ as previously discussed. The matching is successful *only if* the sign of the right-hand side (r.h.s.) of Eq. (24) is positive as originally assumed and only then is the dispersion relation (23) valid. (We arrive at the same condition if we initially assume that Im$\{c\}<0$). It is shown in Appendix B that for $R>2$ (i.e., $\tilde{J}\simeq 0$), the r.h.s. of (24) is always positive and the matching is successful. For the special case, however, in which $R=2$ (i.e., $\tilde{J}=J_\infty$), the matching is not always successful because the product $\Gamma(b)\Gamma(d-a)$ that appears in Eq. (24) can change sign depending on the value of $\tilde{J}$. In particular, it is shown in Appendix B that if $\tilde{J}>2q/(2q+1)^2$, the r.h.s. of Eq. (24) is negative and thus we end up with a contradiction. Therefore, in the $R=2$ case, we have shown instability only if

$$\tilde{J}<2q/(2q+1)^2. \tag{25}$$

Note that the maximum of the right-hand side of Eq. (25) is 1/4, and this condition implies that the Richardson criterion should hold at the location of the critical height $\tilde{J}=\mathrm{Ri}(y_c)<1/4$.

The unsuccessful matching when the condition (25) is not satisfied suggests (but does not prove) that there is no smooth solution that satisfies the TG equation in this limit. However, the TG spectrum does not consist only of smooth modes. There is an infinity of neutral modes with a discontinuity of the first derivative at the critical height and it cannot be considered as the limit of smooth unstable solutions for $\text{Im}\{c\}\to 0$. These modes form the continuous spectrum of the Taylor-Goldstein equation and have been studied before in the literature.[39,40] It is possible, therefore, that the reason there is no successful matching for the modes with $q>q_0$ is that in this region only modes of the continuous spectrum exist. It is also important to emphasize that the lack of instability at this order does not imply stability. Nonzero growth rate of smaller order can still exist and therefore the above result should be interpreted only as a sufficient condition for instability.

To summarize this section, it has been shown that if $R>2$, the modes with phase velocity equal to the maximum phase velocity of the shear are marginally unstable: wavenumbers with $q<q_0$ are stable and wavenumbers with $q>q_0$ are unstable. If $R=2$, these modes are marginally unstable only if the condition (25) is further satisfied and stable (to the examined order) otherwise. The only assumptions that were needed for the proof is that (i) the asymptotic behavior of the velocity and density profile has the exponential behavior described at the beginning of Sec. II, (ii) modes with $c(q)=1$ exist, and (iii) the integral I_2 exists and is finite.

III. MARGINAL *R*

In the preceding section, marginal instability was shown when the wavenumber q is varied from the critical value q_0. However, the wavenumber is not a control parameter in a system. It is desirable, therefore, to examine a system for which one of the control parameters (J_0 or R) is close to the critical value for which the instability begins. Since Holmboe instability is present for arbitrarily large values of J_0, the only other control parameter left is R. It is interesting, therefore, to consider a case for which $R=2+\delta$ with $0<\delta\ll 1$ and the $c=1$ solution (ϕ_0,q_0) is known with q_0 such that $J_\infty>2q_0/(2q_0+1)^2$ so that the $R=2$ case gives no instability at the examined order. We make a small variation in $q=q_0+\epsilon q_1$ and $c=1-\epsilon c_1$ with the exact relation between δ and ϵ still undetermined. At this stage, it is assumed that ϵ is sufficiently smaller than δ so that the procedure in the previous section is still valid, and then the value of ϵ gradually increases until the approximations in the previous section start to fail. As the value of ϵ is increased, the most sensitive term (in ϵ) that will be affected first is the term proportional to $\tilde{J}=J_\infty\cdot(\epsilon c_1/\sigma)^\delta$ in Eq. (15), for which ϵ is raised to the smallest appearing power. Note that if $\epsilon\ll\exp[-1/\delta]$, then $\tilde{J}\ll 1$ and the results of the previous section are still valid. If, however, $\epsilon\sim\mathcal{O}(\exp[-1/\delta])$, then $\tilde{J}\sim\mathcal{O}(1)$. Following the same steps as in the previous section, we end up in the dispersion relation given by Eq. (23), but as in the $R=2$ case, $\tilde{J}$ cannot be treated as a small parameter.

The difference from the $\delta=\mathcal{O}(1)$ case will therefore appear when we try to determine the sign of the r.h.s. of Eq. (24). To have successful matching, we need to satisfy the condition (25). Since $\tilde{J}$ is finite, the condition $\tilde{J}<2q/(2q+1)^2$ that also appears in the $R=2$ case could be violated. To capture the whole unstable region, we define ϵ such that $J_\infty\epsilon^\delta=2q_0/(1+2q_0)^2$ or

$$\epsilon=\left[\frac{2q_0/J_\infty}{(1+2q_0)^2}\right]^{1/\delta}\ll 1. \tag{26}$$

Note that the term inside the brackets is always smaller than 1. For such a choice, the condition (25) for instability reads

$$\tilde{J}=J_\infty\cdot\left(\frac{\epsilon c_1}{\sigma}\right)^\delta=\left[\frac{2q_0}{(1+2q_0)^2}\right][1+\delta\ln(c_1/\sigma)+\mathcal{O}(\delta^2)] < \left[\frac{2q_0}{(1+2q_0)^2}\right]+\mathcal{O}(\epsilon) \tag{27}$$

or $c_1/\sigma<1$. Already at this stage it can be seen that there is instability only if $c_1=2q_1q_0I_1/I_2<\sigma$ and therefore the instability is confined in the region of wavenumbers

$$q_0<q<q_0+\Delta q, \tag{28}$$

where $\Delta q=\epsilon\sigma I_2/2q_0I_1$. Therefore, the second instability boundary for the Holmboe instability is given by $q+\Delta q$. To get the full dispersion relation in this asymptotic limit, we need to expand in terms of δ the product $\Gamma(d-a)\Gamma(b)$ that appears in Eq. (23) since this is the term that can change sign depending on the value of $\tilde{J}$. This is done in Appendix B, and the resulting growth rate inside the instability region to the first nonzero order becomes

$$\zeta=q_0\,\text{Im}\{c\}=-\delta C_1q_0|q_0-q|^{2\lambda}\ln\left(\frac{2(q-q_0)q_0I_1}{\epsilon I_2\sigma}\right), \tag{29}$$

where $C_1>0$ is an $\mathcal{O}(1)$ quantity and is given in Eq. (B1). The maximum of the growth rate is obtained for $q-q_0=\epsilon e^{-1/2\lambda}I_2\sigma/(2q_0I_1)$ with the growth rate being given by

$$\max[\zeta]=\delta\epsilon^{2\lambda}\frac{C_1q_0}{2\lambda e}\left[\frac{I_2\sigma}{q_0I_1}\right]^{2\lambda}. \tag{30}$$

Therefore, the growth rate scales like $\epsilon^{2\lambda}$ and the width of the instability region scales like $\Delta q\sim\epsilon$. In terms of δ, these relations are given by $\zeta\sim\delta e^{-2\lambda\gamma/\delta}$ and $\Delta q\sim e^{-\gamma/\delta}$, where γ is a positive constant. This very strong dependence with δ suggests that both ζ and Δq decrease very rapidly as δ becomes smaller. This can explain the difficulty numerical codes have, when attempting to calculate growth rate for values of R very close to $R=2$.

IV. EXAMPLES

The previous sections presented some general results for the Holmboe unstable modes. This section examines some specific examples often used in the literature to model Holmboe's instability.

Consider first the Hazel model that was introduced in Sec. I. Based on the definitions given in Sec. II, we have that $\alpha=2$, $\beta=2R$, $U^*=2$, and $J_*=4J_0$. The resulting nondimensional quantities are $J_\infty=J_0/4$, $\sigma=2$, $q=k/2$, and R has the same meaning. This model satisfies all the conditions that are stated in Sec. II, therefore for $R>2$ the modes with $c(k)=\pm 1$ are marginally unstable. Furthermore, for the case $R=2$ there is instability only if the condition (25) is satisfied, or in the units of this example if $J_0/4<k/(k+1)^2$. A simple

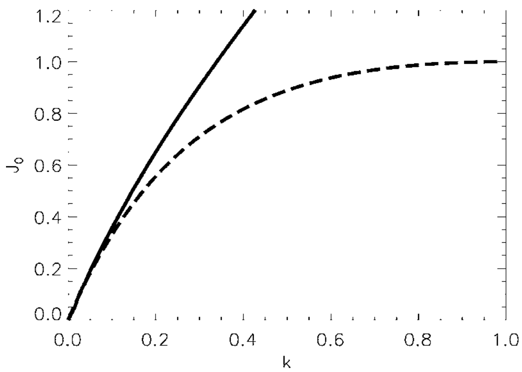

FIG. 3. The $c=1$ solutions for the Hazel model $J_0(k)$ for $R=2$ (solid line), the condition from Eq. (25), $J_0<4k/(k+1)^2$ (dashed line).

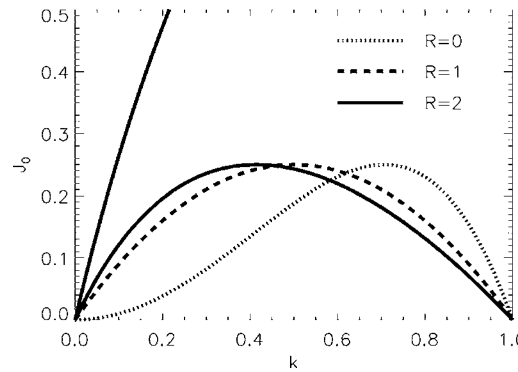

FIG. 5. The $c=1$ and 0 solutions for the model with density stratification given by $J(y)=J_0\cosh^{-2R}(y)$ for $R=0$ (dotted line), $R=1$ (dotted line), and $R=2$ (solid line).

numerical integration shows that this is not the case for this profile (see Fig. 3). Therefore, the $R=2$ is stable (to the examined order) and is the critical value beyond which the Holmboe instability begins. The imaginary part of $c(k)$ for this profile for the case in which $R=2.1$ and $J_0=1.2$ is shown if Fig. 4, where the numerical result is compared with the asymptotic expansion of Eq. (29). Although $\delta=0.1$ is not very small, there is satisfactory agreement (a 20% difference) between the asymptotic and the numerical result. It is worth mentioning that it is very hard to find a range of values of δ in which both the asymptotic result is valid and $\mathrm{Im}\{c\}$ is large enough to be captured by a numerical code. Note that decreasing the value of δ from 0.1 to 0.05 has resulted in a drop of $\mathrm{Im}\{c\}$ by three orders of magnitude.

A second family of flows that is considered in this section assumes a velocity profile given by $U(y)=\tanh(y)$ as in the Hazel model and the density stratification being determined by

$$-g\rho'/\rho=\frac{J_0}{\cosh^{2R}(y)}.$$

The advantage of this profile is that there are analytic solutions for the Kelvin-Helmholtz stability boundaries $J_0(k)$ for the cases in which $R=0$, 1, and 2. These stability boundaries are determined by the neutral modes that have phase velocity equal to the velocity of the flow at the inflection point, i.e., $c(k)=0$. In addition, there is an analytic solution $J_0(k)$ for the modes k for which $c(k)=1$ for the $R=2$ case. The $R=0$ case

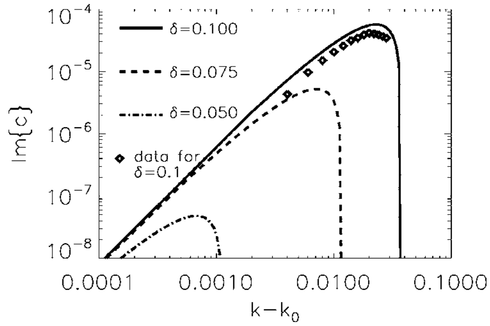

FIG. 4. The $\mathrm{Im}\{c\}$ for the Hazel model for $R=2+\delta$ with $\delta=0.1,0.75,0.05$ and $J_0=1.2$. The diamonds indicate the results from numerical integration for the $\delta=0.1$ case.

was examined in Ref. 41, in which it was shown that the Kelvin-Helmholtz unstable modes satisfy $J_0<k^2(1-k^2)$. The $R=1$ case (which reduces to the $R=1$ case of the Hazel model) was investigated in Ref. 35, in which it was shown that the Kelvin-Helmholtz unstable modes satisfy $J_0<k(1-k)$. The $R=2$ case has not been investigated before (to the author's knowledge). One can show following the same methods used for the $R=0,1$ cases[35,41,42] that the $c(k)=0$ modes satisfy

$$J_0=\frac{k(1-k)(2+k)(3+k)}{4(k+1)^2}$$

with $\phi(y)=[1-\tanh(y)^2]^{k/2}\cdot[\tanh(y)]^{1/4-\sqrt{1/4-J_0}}$ and provide the Kelvin-Helmholtz instability boundary. The $c(k)=1$ modes, on the other hand, that are of interest for the Holmboe instability satisfy

$$J_0=\frac{k(3+2k)}{(k+1)^2}$$

for $k<1$. The stream function ϕ for these modes is given by $\phi=[1+\tanh(y)]^{k/2}\cdot[1-\tanh(y)]^{\sqrt{k^2/4+1-J_0}}$. The Kelvin-Helmholtz stability boundaries for the three cases $R=0,1,2$ along with the $c=1$ solutions for the $R=2$ case are shown in Fig. 5. For this example, $\sigma=2$ and $q=k/2$ and $J_\infty=2^{2R-4}J_0$. The $J_0(k)$ relation for the $c=1$ solutions does not satisfy the criterion (25), which now reads $J_0<k/(k+1)^2$, thus the $R=2$ case is stable (to the examined order) and is the critical value above which the Holmboe instability begins. Because J_∞ is four times bigger than in the Hazel model (for the same J_0), the resulting growth rate is smaller by a factor of $4^{-2\lambda/\delta}$, which is close to 10^{-14} for the $\delta=0.1$ case. Figure 6 shows the growth rate based on the asymptotic expansion (29). No numerical results could be obtained for this case for values of $\delta\leqslant 0.1$ that would justify a comparison with the asymptotic expansion. This example, when compared with one of Hazel, clearly demonstrates the sensitivity of the resulting growth rate to the large y asymptotic behavior of $J(y)$ and $U(y)$: a change by a factor of 4 in J_∞ resulted in a 14 orders of magnitude difference in the growth rate.

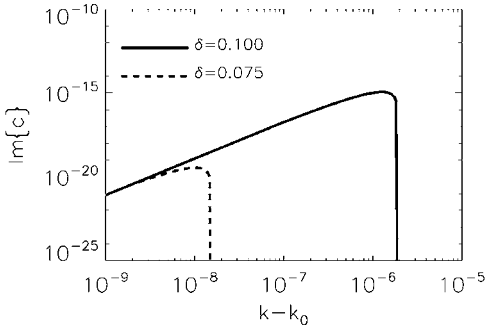

FIG. 6. The $\mathrm{Im}\{c\}$ for the $J(y)=J_0\cosh^{-2R}(y)$ model for $J_0=1.2$ and $R=2+\delta$ with $\delta=0.1$ (solid line) and $\delta=0.075$ (dashed line).

V. CONCLUSIONS

In this paper, Holmboe's instability for smooth density and velocity profiles is examined analytically. It is shown for a large family of flows that the modes with phase velocity equal to the maximum or minimum of the unperturbed velocity profile when they exist, and if the parameter R is above the critical value ($R_{\mathrm{crit}}=2$) they constitute a stability boundary. This result confirms the results obtained numerically in Ref. 17, where the fact that the $c=U_{\mathrm{max/min}}$ modes are marginally unstable was only conjectured based on physical arguments and numerical results. It is also the first time shown analytically that the value of $R=2$ for the Hazel model is the critical value R_{crit} above which the Holmboe instability begins.

For the case in which the parameter R is only slightly larger than its critical value $R_{\mathrm{crit}}=2$, the dispersion relation $c(k)$ was obtained based on an asymptotic expansion. For this marginally unstable flow, the growth rate ζ as well as the width of the instability stripe Δq have a very strong dependence on the deviation of R from its critical value. In particular, the growth rate ζ and the width of the instability Δk scale as $\exp[-2\lambda\gamma/(R-R_{\mathrm{crit}})]$ and $\exp[-\gamma/(R-R_{\mathrm{crit}})]$, respectively (for some positive constant γ). For this reason, the numerical investigations performed in the past[16,17] were not able to capture the instability for values of R very close to R_{crit}.

The author believes also that the present results go beyond the clarification of a mathematical detail in the literature. They demonstrate the mechanisms involved in the Holmboe instability in a quantitative way, for the limit examined in this paper. In physical terms, one recognizes two regions that are important. First there is the region $y=\mathcal{O}(1)$ that determines to first order the real part of the phase velocity of the gravity waves (i.e., the correction c_1' of order ϵ). The gravity waves are coupled to the critical layer that appears at the height at which the velocity of the shear is equal to the phase velocity of the gravity waves. The location of the critical layer for an unstable gravity wave mode has to be at large enough heights so that the shear strain can overcome stratification. One would then expect that the height of the critical layer would be such that $\mathrm{Ri}(y_c)<1/4$. [Note that for the cases examined, $\mathrm{Ri}(y)\sim J_\infty e^{-\delta y}$. This restricts y_c to the range $\ln(4J_\infty)/\delta\lesssim y_c$ and can be very large.] The growth rate of the mode will then strongly depend on the properties of the shear at this height (i.e., the correction c_2' of order $\epsilon^{2\lambda}$). The coupling between the critical layer and the gravity wave gives rise to the instability. This necessary coupling between the gravity wave and the critical layer restricts the unstable wavenumbers in the following way. If the wavenumber is too small, the gravity wave travels faster than the shear velocity and there is no height y_c such that $U(y_c)=c$, no critical layer will be formed, and the gravity wave will be stable. If the wavenumber is too large, the gravity wave is slow and the critical layer forms in small heights such that $\mathrm{Ri}(y)>1/4$, the shear strain will not be able to overcome the stratification, and as a result the gravity wave will be stable again. Therefore, unstable wavenumbers are only the ones whose phase speed is smaller than U_{max} but large enough so that the critical layer is formed in the $\mathrm{Ri}(y)<1/4$ region. As the parameter R approaches from above the critical value $R_{\mathrm{crit}}=2$, the smallest allowed height of the critical layer becomes larger and as a result the range of allowed wavenumbers for Holmboe's instability becomes smaller and the growth rate is decreased.

For example, for the density and velocity profiles considered in this paper, if the phase speed of a mode close to the critical wavenumber q_0 can be written in terms of a Taylor expansion as $c(q_0+\Delta q)\simeq 1+a_1\Delta q+\cdots$ (with $a_1=[\partial_q c(q)]_{q=q_0}<0$), the unstable wavenumbers will be restricted in two ways. First, Δq must be positive ($\Delta q>0$) so that the phase velocity is smaller than 1. Second, the condition $\mathrm{Ri}(y_c)\sim J_\infty e^{-\delta y_c}<1/4$ needs to be satisfied. The critical layer will form at a height $y_c\sim -\ln(a_1\Delta q)$ where the behavior $U(y)\simeq 1-e^{-y}$ is assumed again. This leads us to the estimate $\Delta q\lesssim a_1^{-1}[4J_\infty]^{-1/\delta}$.

Furthermore, as the critical layer moves at larger heights, its coupling with the gravity wave becomes weaker. How weak this coupling is will depend on the amplitude of the gravity wave mode at the critical height. If we estimate the critical height by $\mathrm{Ri}(y_c)\simeq J_\infty e^{-\delta y}\sim r$ (for some r in the range $0<r<1/4$), and taking into account that $\phi\sim e^{-\lambda y}$ for large y leads to an estimate of the growth rate $\zeta\sim e^{-\lambda y_c}\sim[r/J_\infty]^{-\lambda/\delta}$. The scaling that we get for Δq and ζ as a function of J_∞ and δ with these simple phenomenological arguments is exactly the same with the scalings that were obtained in the detailed calculation. Although these phenomenological estimates should not be trusted to a large extent, they can provide a first order of magnitude estimate of the expected unstable wavenumbers and their growth rates, in situations where the exact functional form of the density stratification and the velocity profile are not precisely known, as in experiments, and in geophysical and astrophysical flows.

Finally, it is the author's belief that the results given in this paper can provide a basis for further numerical and analytical investigations such as an examination of the weakly nonlinear theory where a small nonlinearity is taken into account in order to examine the long time evolution of an unstable mode beyond the linear stage.

ACKNOWLEDGMENTS

Most of this work was done while the author was at ASP post-doc at the National Center for Atmospheric Research

(NCAR), and the support is gratefully acknowledged. Present support by the Observatory of Nice (Observatoire de la Côte d'Azur) that helped the author finish this work is also acknowledged. The author would also like to thank the two anonymous referees whose suggestions helped to improve this paper.

APPENDIX A: THE HYPERGEOMETRIC EQUATION: BASIC PROPERTIES

The hypergeometric equation is

$$z(1-z)\frac{d^2f}{dz^2}+[d-(a+b+1)z]\frac{df}{dz}-abf=0. \tag{A1}$$

The solution that remains finite as $z\to 0$ is the hypergeometric function, $f=F(a,b,c;z)$. For the normalization condition we are using, we have the following limits:

$$\lim_{z\to 0} F(a,b,c;z)=1/\Gamma(d),$$

$$\lim_{z\to 1} F(a,b,c;z)\simeq\frac{\Gamma(d)\Gamma(d-a-b)}{\Gamma(d-a)\Gamma(d-b)}+\frac{\Gamma(d)\Gamma(a+b-d)}{\Gamma(a)\Gamma(b)}(1-z)^{d-a-b},$$

$$\lim_{z\to +\infty} F(a,b,c;z)\simeq\frac{\Gamma(d)\Gamma(b-a)}{\Gamma(b)\Gamma(d-a)}(-z)^{-a}-\frac{\Gamma(d)\Gamma(a-b)}{\Gamma(a)\Gamma(d-b)}(-z)^{-b}$$

provided that $d\neq 0,-1,-2,\ldots$ and $a-b$ is not an integer.

APPENDIX B: THE SIGN OF THE INSTABILITY TERM

To determine whether we have successful matching, we need to find the sign of the imaginary part in the dispersion relation (23). We examine each term separately. Clearly, $\Gamma(a)$, $\Gamma(2\lambda)$, and $\Gamma(d-b)$ are all positive factors since the argument of the Γ function is positive. The factor $\Gamma(-2\lambda)$ is changing sign every time 2λ is an integer. However, its product with $\sin(2\lambda\pi)$ always remains negative. The factors $\Gamma(b)$ and $\Gamma(d-a)$, however, can change sign depending on the value of $\tilde{J}$. Using the expressions for a,b,d, one can show that $-1\leqslant b\leqslant 0$ if $\tilde{J}\leqslant(2q)/(2q+1)^2$ or if $2q\leqslant 1$, and positive otherwise. Similarly, we have that $-1\leqslant d-a<0$ if $\tilde{J}>(2q)/(2q+1)^2$ and $2q<1$ and non-negative otherwise. Combining these two inequalities, we can determine the sign of the product

$$\Gamma(b)\Gamma(d-a)\leqslant 0 \quad \text{if and only if} \quad \tilde{J}\leqslant(2q)/(2q+1)^2.$$

The result in (24) then follows.

To find the dispersion relation for the small δ and ϵ given by (26), we need to find an expression for the term $\Gamma(b)\Gamma(d-a)$. Substituting the choice of ϵ given by (26) in the expression for b and $d-a$ and using $\tilde{J}=J_\infty(\epsilon c_1/\sigma)^\delta\simeq J_\infty(\epsilon)^\delta[1+\delta\ln(c_1/\sigma)]$, we have that to first order in δ if $2q_0>1$,

$$b\simeq\frac{1}{2}\delta J_\infty\epsilon^\delta\ln(c_1/\sigma)\left[\frac{1}{\sqrt{1/4-J_\infty\epsilon^\delta}}+\frac{1}{\sqrt{1+q_0-J_\infty\epsilon^\delta}}\right]$$

and $b=\mathcal{O}(1)$ if $2q_0<1$. Similarly,

$$d-a\simeq\frac{1}{2}\delta J_\infty\epsilon^\delta\ln(c_1/\sigma)\left[\frac{1}{\sqrt{1/4-J_\infty\epsilon^\delta}}+\frac{1}{\sqrt{1+q_0-J_\infty\epsilon^\delta}}\right]$$

if $2q<1$ and $d-a=\mathcal{O}(1)$ if $2q>1$. Using the Γ-function property $\Gamma(\delta)=\Gamma(1+\delta)/\delta$, we can write the dispersion relation for $q_0<q<q_0+\epsilon\sigma I_2/k_0I_1$ as

$$c=1-2(q-q_0)q_0I_1/I_2+\delta C_1(q_0-q)^{2\lambda}\ln\left(\frac{2(q-q_0)q_0I_1}{I_2\sigma}\right),$$

where

$$C_1=\frac{J_\infty\epsilon^\delta\lambda\varphi_\infty^2}{I_2}\left(\frac{2q_0I_1}{I_2}\right)^{2\lambda}\frac{\sin(2\lambda)\Gamma(a)\Gamma(d-b)\Gamma(-2\lambda)}{\Gamma(w)\Gamma(2\lambda)}\times\left[\frac{1}{\sqrt{1/4-J_\infty\epsilon^\delta}}+\frac{1}{\sqrt{1+q_0-J_\infty\epsilon^\delta}}\right] \tag{B1}$$

with $w=b$ if $2q_0<1$ and $w=d-a$ if $2q_0>1$.

[1]R. Rosner, A. Alexakis, Y. Young, J. Truran, and W. Hillebrand, "On the C/O enrichment of novae ejecta," Astrophys. J. Lett. **562**, L177 (2002).
[2]A. Alexakis, A. C. Calder, A. Heger, E. F. Brown, L. J. Dursi, J. W. Truran, R. Rosner, D. Q. Lamb, F. X. Timmes, B. Fryxell, M. Zingale, P. M. Ricker, and K. Olson, "On heavy element enrichment in classical novae," Astrophys. J. **603**, 931 (2004).
[3]D. M. Farmer and H. Freeland, "The physical oceanography of fjords," Prog. Oceanogr. **12**, 147 (1983).
[4]G. Pawlak and L. Armi, "Hydraulics of two-layer arrested wedge flows," J. Hydraul. Res. **35**, 603 (1997).
[5]L. Armi and D. M. Farmer, "The flow of Mediterranean water through the Strait of Gibraltar," Prog. Oceanogr. **21**, 1 (1988).
[6]T. Oguz, E. Ozsoy, M. A. Latif, H. I. Sur, and U. Unluata, "Modeling of hydraulically controlled exchanged flow in the Bosphorous Strait," J. Phys. Oceanogr. **20**, 945 (1990).
[7]F. E. Sargent and G. H. Jirka, "Experiments on saline wedge," J. Hydraul. Eng. **113**, 1307 (1987).
[8]S. Yoshida, M. Ohtani, S. Nishida, and P. F. Linden, "Mixing processes in a highly stratified river," *Physical Processes in Lakes and Oceans*, edited by J. Imberger (American Geophysical Union, Washington, DC, 1998).
[9]P. Pettre and J. C. Andre, "Surface-pressure change through Loewe's phenomena and katabatic flow jumps. Study of two cases in Adelie Land Antarctica," J. Atmos. Sci. **48**, 557 (1991).
[10]J. Holmboe, "On the behavior of symmetric waves in stratified shear layers," Geophys. Publ. **24**, 67 (1962).
[11]G. A. Lawrence, F. K. Browand, and L. G. Redekopp, "The stability of a sheared density interface," Phys. Fluids A **3**, 2360 (1991).
[12]C. P. Caulfield, "Multiple linear instability of layered stratified shear flow," J. Fluid Mech. **258**, 255 (1994).
[13]S. P. Haigh and G. A. Lawrence, "Symmetric and non-symmetric Holmboe instabilities in an inviscid flow," Phys. Fluids **11**, 1459 (1999).
[14]S. Ortiz, J. M. Chomaz, and T. Loiseleux, "Spatial Holmboe instability," Phys. Fluids **14**, 2585 (2002).

[15] S. P. Hazel, "Numerical studies of the stability of inviscid shear flows," J. Fluid Mech. **51**, 3261 (1972).
[16] W. D. Smyth and W. R. Peltier, "The transition between Kelvin-Helmholtz and Holmboe instability: An investigation of the over-reflection hypothesis," J. Atmos. Sci. **46**, 3698 (1989).
[17] A. Alexakis, "On Holmboe's instability for smooth shear and density profiles," Phys. Fluids **17**, 084103 (2005).
[18] S. Nishida and S. Yoshida, "Stability and eigenfunctions of disturbances in stratified two layer shear flow," *Proceedings of the Third International Symposium on Stratified Flows, Pasadena, CA, 1987* (ASCE, New York, 1990), pp. 28–34.
[19] W. D. Smyth and W. R. Peltier, "Three-dimensional primary instabilities of a stratified dissipative, parallel flow," Geophys. Astrophys. Fluid Dyn. **52**, 249 (1990).
[20] W. D. Smyth, G. P. Klaasen, and W. R. Peltier, "Finite amplitude Holmboe waves," Geophys. Astrophys. Fluid Dyn. **43**, 181 (1988).
[21] W. D. Smyth and W. R. Peltier, "Instability and transition in finite amplitude Kelvin-Helmholtz and Holmboe waves," J. Fluid Mech. **228**, 387 (1991).
[22] B. R. Sutherland, C. P. Caulfield, and W. R. Peltier, "Internal gravity generation and hydrodynamic instability," J. Atmos. Sci. **51**, 3261 (1994).
[23] A. Alexakis, A. C. Calder, L. J. Dursi, R. Rosner, J. W. Truran, B. Fryxell, M. Zingale, F. X. Timmes, K. Olson, and P. Ricker, "On the nonlinear evolution of wind-driven gravity waves," Phys. Fluids **16**, 3256 (2004).
[24] W. D. Smyth and K. B. Winters, "Turbulence and mixing in Holmboe waves," J. Phys. Oceanogr. **33**, 694 (2003).
[25] F. K. Browand and C. D. Winant "Laboratory observations of shear layer instability in a stratified fluid," Boundary-Layer Meteorol. **5**, 67 (1973).
[26] C. G. Koop, "Instability and turbulence in a stratified shear layer," Tech. Rep. USCAE 134, Department of Aerospace Engineering, University of Southern California (1976).
[27] G. Pawlak and L. Armi, "Vortex dynamics in a spatially accelerating shear layer," J. Fluid Mech. **376**, 1 (1999).
[28] O. Pouliquen, J. M. Chomaz, and P. Huerre, "Propagating Holmboe waves at the interface between two immiscible fluids," J. Fluid Mech. **266**, 277 (1994).
[29] D. Z. Zhu and G. A. Lawrence, "Holmboe's instability in exchange flows," J. Fluid Mech. **429**, 391 (2001).
[30] A. M. Hogg and G. N. Ivey, "The Kelvin-Helmholtz to Holmboe instability transition in stratified exchange flows," J. Fluid Mech. **477**, 339 (2003).
[31] N. Yonemitsu, G. E. Swaters, N. Rajaratnam, and G. A. Lawrence "Shear instabilities in arrested salt wedge flows," Dyn. Atmos. Oceans **24**, 173 (1996).
[32] C. P. Caulfield, W. R. Peltier, S. Yoshida, and M. Ohtani, "An experimental investigation of the instability of a shear flow with multi-layered density stratification," Phys. Fluids **7**, 3028 (1995).
[33] P. G. Drazin and W. H. Reid, *Hydrodynamic Stability* (Cambridge University Press, Cambridge, UK, 1981).
[34] L. N. Howard, "A note on a paper of John Miles," J. Fluid Mech. **10**, 509 (1961).
[35] J. Miles, "On the stability of heterogeneous shear flow. Part 2," J. Fluid Mech. **16**, 209 (1963).
[36] A. Alexakis, Y. Young, and R. Rosner, "Shear instability of fluid interfaces: A linear analysis," Phys. Rev. E **65**, 026313 (2002).
[37] A. Alexakis, Y. Young, and R. Rosner, "Weakly non-linear analysis of wind driven gravity waves," J. Fluid Mech. **503**, 171 (2004).
[38] S. M. Churilov, "Stability analysis of stratified shear flows with a monotonic velocity profile without inflection points," J. Fluid Mech. **539**, 25 (2005).
[39] W. H. H. Banks, P. G. Drazin, and M. B. Zaturska, "On the normal modes of parallel flow of inviscid stratified fluid," J. Fluid Mech. **75**, 149 (1976).
[40] N. J. Balmforth and P. J. Morrison, "Normal modes and continuous spectra," Ann. N.Y. Acad. Sci. **773**, 80 (1995).
[41] P. G. Drazin, "The stability of a shear layer in an unbounded heterogeneous inviscid fluid," J. Fluid Mech. **4**, 214 (1958).
[42] L. N. Howard, "Neutral curves and stability boundaries in stratified shear flow," J. Fluid Mech. **16**, 333 (1963).